# Enhanced second-harmonic generation by means of high-power confinement in a photovoltaic soliton-induced waveguide

**Cibo Lou, Jingjun Xu, Haijun Qiao, Xinzheng Zhang, and Yunlin Chen**

*TEDA Applied Physics School, Nankai University, Tianjin 300457, China, and Photonics Center, College of Physics Science, Nankai University, Tianjin 300071, China*

**Zhigang Chen**

*Department of Physics and Astronomy, San Francisco State University, and TEDA Applied Physics School, Nankai University, Tianjin 300457, China*

Received September 25, 2003

We present the first experimental demonstration of enhanced second-harmonic generation (SHG) by means of power confinement with a femtosecond laser in a photovoltaic soliton-induced waveguide. A dark spatial soliton created with a weak cw laser beam in a photovoltaic lithium niobate crystal induces an efficient waveguide for SHG, leading to a 60% enhancement of the conversion efficiency. © 2004 Optical Society of America

*OCIS codes:* 190.0190, 190.2620, 190.5530.

Since the first prediction[1] and observation[2] of photorefractive spatial solitons, their potential applications in waveguiding,[3,4] directional coupling,[5] electro-optical switching,[6] and frequency conversion[7] have attracted considerable interest. This is in part due to the unique properties of photorefractive solitons, such as low-power requirements and wavelength sensitivity. Furthermore, the ability to control an intense light beam with a relatively weak beam can be realized in waveguides induced by photorefractive solitons. Among these applications, nonlinear frequency conversion in a waveguide induced by spatial photorefractive solitons is of particular interest. As demonstrated experimentally by Lan *et al.*,[7] second-harmonic generation (SHG) showed an improved conversion efficiency in a waveguide induced by a bright photorefractive-screening soliton compared with the same process in a bulk crystal of $KNbO_3$, which was later analyzed theoretically.[8] In addition, Lan *et al.* studied the tuning of SHG in a waveguide induced by photorefractive solitons.[9] It was also suggested that the tunability of frequency conversion could be increased greatly should a dark soliton-induced waveguide be used.[4,10] However, to our knowledge, since that first demonstration of SHG with a bright soliton waveguide in $KNbO_3$ crystals, no further experimental study of frequency conversion based on light self-waveguiding has been performed.

Lithium niobate crystals ($LiNbO_3$) are versatile nonlinear optical materials. In particular, quasi-phase-matched SHG in periodically poled $LiNbO_3$ crystals was recently investigated widely, because of the feasibility of periodic poling in such crystals.[11] Spatial solitons have also been predicted to exist in quasi-phase-matched quadratic crystals,[12] whereas photovoltaic solitons and soliton-induced waveguides have been demonstrated in $LiNbO_3$ crystals.[13–15] All this shows that $LiNbO_3$ crystals are promising for applications in multimode and multiwavelength light transporting. Therefore it is natural to ask whether efficient nonlinear frequency conversion can be realized in $LiNbO_3$ based on soliton-induced waveguides. In this Letter we demonstrate experimentally the enhancement of SHG by means of high-power confinement in a photovoltaic soliton-induced waveguide in $LiNbO_3$. A 60% enhancement of the conversion efficiency for SHG is achieved.

Our experimental setup is shown in Fig. 1. A laser beam at 532 nm from a frequency-doubled Nd:YAG was selected to construct the dark spatial soliton in $LiNbO_3$. Half of a thin glass sheet was inserted into the expanded laser beam. By tilting the thin glass, we created a phase step between the two parts of the beam, which gave rise to a dark notch necessary for the formation of dark solitons. The dark notch was then imaged by cemented double lens $L_1$ ($f = 50$ mm) onto the input face of our sample (a $LiNbO_3$ crystal doped with 0.03-wt./% Fe; $a \times b \times c \sim 10$ mm $\times$ 10 mm $\times$ 10 mm). A femtosecond laser pulse was used as the fundamental (FM) frequency beam to realize SHG to avoid destroying the light-induced waveguide, because its pulse duration is far shorter than the thermal and photorefractive response of the sample. In addition, its large spectrum width (~10 nm) is also expected to reduce the influence resulting from the phase mismatch in light diffraction. In our experiment the femtosecond laser beam (800 nm) was focused by a cylindrical lens into the dark notch at the input face of the crystal. Another cemented double lens $L_2$ ($f = 60$ mm) was employed to image the input and output faces of the crystal onto a CCD camera. Because the second-harmonic (SH) and the FM beams propagate in the same direction, a dispersion prism

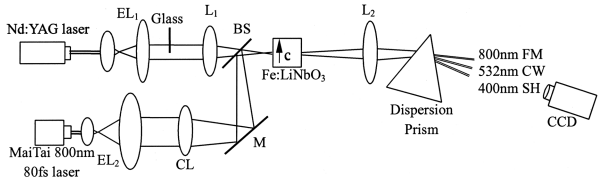


Fig. 1. Experimental setup: $EL_1$, $EL_2$, extender lens; $L_1$, $L_2$, lens; CL, cylindrical lens; M, mirror; BS, beam splitter.

0146-9592/04/090953-03$15.00/0 

was used to separate them. The dark notch was perpendicular to the crystalline $c$ axis, so the orientation of the induced index gradient was along the $c$ axis. The notch-bearing beam, extraordinarily polarized, creates an index change along the $c$ axis through the electro-optic effect induced by the photovoltaic field. This index change is responsible for the self-trapping of light and formation of the photovoltaic soliton.[10]

Typical experimental results are presented in Fig. 2. The dark notch has a width of 18 $\mu$m (FWHM) at the input face of the crystal (Fig. 2a), and it diffracts to 40 $\mu$m after 10 mm of propagation through the crystal (Fig. 2b). At room temperature a steady-state dark soliton was obtained after 12 min of illumination with the dark-notch-bearing beam with its intensity of $\sim$33.6 mW/cm$^2$, as shown in Fig. 2c. Such a dark soliton self-induced a waveguide that can be used to guide another beam.[14] A cylindrically focused He–Ne laser beam at 632.8 nm was introduced to test the quality of the induced waveguide. The width of the probe beam at the input face was 26 $\mu$m. Before and after the dark soliton-induced waveguide formation, its width changed from 52 to 25 $\mu$m at the output face, indicating a photovoltaic dark soliton-induced waveguide was formed in the $LiNbO_3$ crystal.

We then launched a femtosecond laser pulse with a wavelength of 800 nm into the dark soliton-induced waveguide. Its pulse duration was $\sim$130 fs, and the repetition rate was 1 kHz, with a single-pulse energy of the order of microjoules. The vertically input beam had a spatial width of 30 $\mu$m (FWHM) (Fig. 2d) and an intensity of 12 W/cm$^2$. Before the waveguide was formed, the output FM beam and the SH beam, both extraordinarily polarized, had powers of 1.22 mW and 125 nW, respectively, and widths of 87 $\mu$m (Fig. 2e) and 120 $\mu$m (Fig. 2g), respectively. Here we define the SHG conversion efficiency as $I_{SH}[1/(I_{SH} + I_{FM})^2] \times 100\%$, where $I_{SH}$ ($I_{FM}$) is the intensity of the SH (FM) beam at the output face. According to the definition, the calculated conversion efficiency is 8.4%/W in the absence of the photovoltaic soliton-induced waveguide. This measurement was done instantaneously after the fundamental beam was launched, so that no photorefractive effect caused by the charge redistribution spatially induced by the FM and SH beams could take place. Then we launched the 532-nm dark-notch-bearing beam to form the $(1 + 1)D$ dark soliton and adjusted the bright stripe of the FM beam into the dark notch. We turned on the fundamental frequency beam in a short interval from time to time to avoid damaging the waveguide.[16] After illuminating the crystal by the dark-notch-bearing beam for 12 min, both the FM and the SH beams were effectively guided by the photovoltaic dark soliton-induced waveguide, as shown in Figs. 2f and 2h. The output power of the SH beam increased to 199 nW. In this case the conversion efficiency was calculated to be 13.4%/W, which showed a 60% improvement due to the formation of a waveguide. This result agrees well with the prediction shown in Fig. 1b of Ref. 7 (in our case $L/z_0$, as defined in Ref. 7, is equal to 1.4). The temporal response of the SH output power was also measured and is illustrated in Fig. 3, showing an increase in the conversion efficiency after the formation of the photovoltaic dark spatial soliton.

As is well known, when an 800-nm beam is launched into $LiNbO_3$ along the $b$ axis, it is impossible to realize phase matching (either type I or type II) of SHG. However, our experimental results definitely show the enhancement of SHG conversion. We think the key reason in our experiment is the high-power confinement effect. The FM beam confined in the narrow channel guide gives rise to surprisingly large intensities in the waveguide, which is enough to produce high conversion efficiency of SHG, even under phase-mismatching conditions. Meanwhile, the optical field confinement of both FM and SH beams in the waveguide limits them from dispersing in space and prolongs the coupling length scale. In addition, there may be other reasons for our observed SHG enhancement. A limitation for SHG is the phase mismatching. In bulk materials the effect of phase mismatching is to limit high conversion efficiencies to a small length scale. Fortunately, the dispersive characteristics of a confined electromagnetic wave in a waveguide differ considerably from those associated with plane wave propagation in the same bulk material, because of the dependence of a confined electromagnetic wave in a waveguide on the geometric properties of the waveguide. This difference may

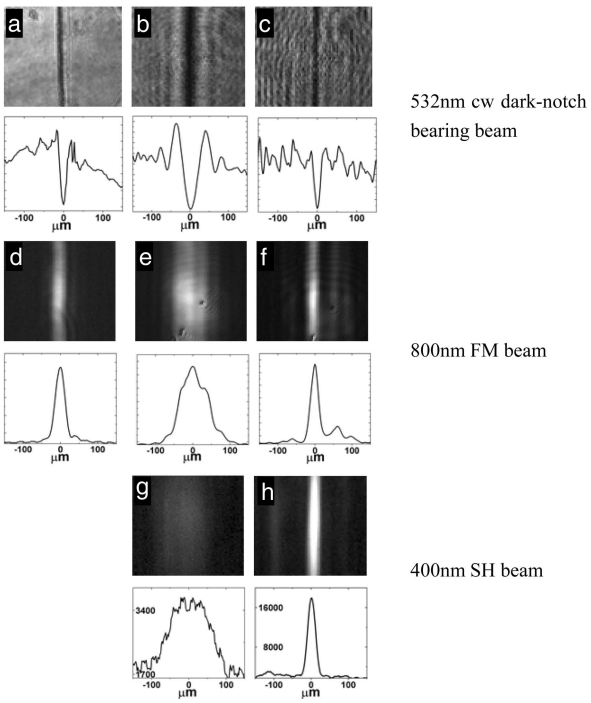


Fig. 2. Experimental result: a, input 532-nm background beam; b, output 532-nm background beam before photovoltaic dark soliton formation; c, output 532-nm $(1 + 1)D$ dark soliton; d, input 800-nm femtosecond bright line; e, output 800-nm femtosecond bright line before photovoltaic dark soliton formation; f, output 800-nm femtosecond bright line guided by the dark soliton-induced waveguide; g, output 400-nm SH bright line before photovoltaic dark soliton formation; h, output 400-nm SH beam guided by the dark soliton-induced waveguide.

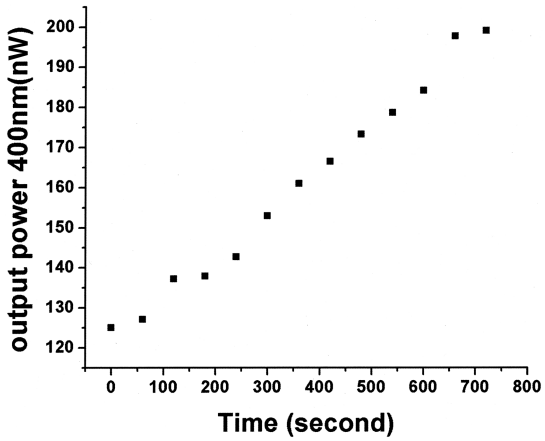


Fig. 3. Temporal response of the SH power with the dark-notch-bearing beam on.

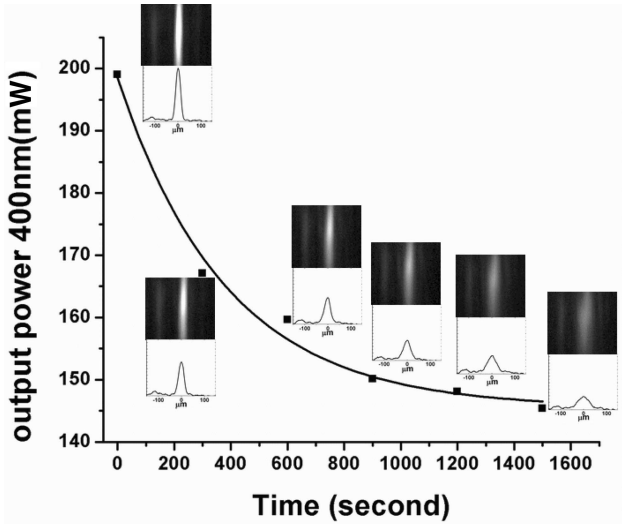


Fig. 4. Filled squares are the temporal response of the SH power during the waveguide erasure with only the 800-nm beam on. The solid curve is the exponential fitting.

suppress the phase mismatch and cause the high conversion efficiency to a larger length scale in the photovoltaic photorefractive soliton-induced waveguide than that in the bulk materials, which will also result in the enhancement of SHG conversion.

Finally, we investigate the damage caused by the conversion process itself to the light-induced waveguide. The femtosecond pulse laser has a very high peak value of energy, and optical damage to $LiNbO_3$ occurs both at 800 (Ref. 16) and 400 nm. We block the dark-notch-bearing beam and keep the FM beam on, so that the induced waveguide is exposed to only FM and SH illumination. The temporal response of the SH output power and transverse intensity profile are shown in Fig. 4. From this figure we can see that, after 25 min, the conversion efficiency reduced to the same level as when the crystal had been illuminated for ~4 min by the dark-notch-bearing beam.

In summary, we have demonstrated the enhancement of SHG of a femtosecond laser beam in a photovoltaic dark soliton-induced waveguide generated with a weak continuous wave in an iron-doped $LiNbO_3$ crystal. The conversion efficiency of SHG in the photovoltaic spatial soliton-induced waveguide is improved significantly by the high-power confinement effect. As future work, we expect more significant results in a vortex waveguide for SHG[17] as well as in waveguides in quasi-phase-matched quadratic crystals such as periodically poled $LiNbO_3$ to combine the high-power confinement effect and the phase-matching condition.

This work was sponsored by the Chinese 973 project (G1999033004) and the National Science Foundation (6010801 and 60328406). We thank the referees for their valuable suggestions. J. Xu's e-mail address is jjxu@nankai.edu.cn.

## References

1. M. Segev, B. Crosignani, A. Yariv, and B. Fischer, Phys. Rev. Lett. **68,** 923 (1992).
2. G. Duree, J. L. Shultz, G. Salamo, M. Segev, A. Yariv, B. Crosignani, P. DiProto, E. Sharp, and R. R. Neurgaonkar, Phys. Rev. Lett. **71,** 533 (1993).
3. M. Morin, G. Duree, G. Salamo, and M. Segev, Opt. Lett. **20,** 2066 (1995).
4. M. Shih, Z. Chen, M. Mitchell, M. Segev, H. Lee, R. S. Feigelson, and J. P. Wilde, J. Opt. Soc. Am. B **14,** 3091 (1997).
5. S. Lan, E. DelRe, Z. Chen, M. Shih, and M. Segev, Opt. Lett. **24,** 475 (1999).
6. E. DelRe, B. Crodignani, P. D. Porto, E. Palange, and A. J. Agranat, Opt. Lett. **27,** 2188 (2002).
7. S. Lan, M. Shih, G. Mizell, J. A. Giordmaine, Z. Chen, C. Anastassiou, J. Martin, and M. Segev, Opt. Lett. **24,** 1145 (1999).
8. A. D. Boardman, W. Ilecki, and Y. Liu, J. Opt. Soc. Am. B **19,** 832 (2002).
9. S. Lan, C. Anastassiou, M. Segev, M. Shih, J. A. Giordmaine, and G. Mizell, Appl. Phys. Lett. **77,** 2101 (2000).
10. G. C. Valley, M. Segev, B. Crosignani, A. Yariv, M. M. Fejer, and M. C. Bashaw, Phys. Rev. A **50,** R4457 (1994).
11. R. G. Batchko, M. M. Fejer, R. L. Byer, D. Woll, R. Wallenstein, V. Y. Shur, and L. Erman, Opt. Lett. **24,** 1293 (1999).
12. N. C. Panoiu, D. Mihalache, D. Mazilu, F. Lederer, and R. M. Osgood, Jr., Phys. Rev. E **68,** 016608 (2003).
13. M. Segev, G. C. Valley, M. C. Bashaw, M. Taya, and M. M. Fejer, J. Opt. Soc. Am. B **14,** 1772 (1997).
14. M. Taya, M. C. Bashaw, M. M. Fejer, M. Segev, and G. C. Valley, Phys. Rev. A **52,** 3095 (1995).
15. M. Segev, M. Shih, and G. Valley, J. Opt. Soc. Am. B **13,** 706 (1996).
16. Q. Wu, J. Xu, G. Zhang, L. Zhao, X. Zhang, H. Qiao, Q. Sun, W. Lu, G. Zhang, and T. R. Volk, Opt. Mater. **23,** 277 (2003).
17. J. R. Salgueiro, A. H. Carlsson, E. Ostrovskaya, and Y. Kivshar, *arXiv.org e-Pring archive*, nlin.PS/309059v1, September 23, 2003, http://arxiv.org/abs/nlin.PS.309059v1.